

## ANALYSIS OF THE POSITIONING SYSTEM FOR CONNECTING PANEL FACES OF TROUGH SOLAR COLLECTOR BRACKETS

Lingzhi YAN<sup>1\*</sup>, Wenbo HUANG<sup>2</sup>, Jiaming WANG<sup>3</sup>, Lanxin HOU<sup>4</sup>, Yonghui LIU<sup>5</sup>, Jianjun WANG<sup>6</sup>

*This paper introduces an industrial camera positioning system for the connecting plate surface of a trough solar collector bracket. The system integrates a high-precision industrial camera, an image processing algorithm, and a precision mechanical control mechanism, aiming at realizing the accurate positioning and detection of the connecting plate surface of the trough solar collector bracket. By capturing high-definition images of the connecting plate surface with the industrial camera, combined with advanced image processing technology, the system can automatically identify the key feature points of the plate surface, thus realizing millimeter-level precision position feedback. The system enhances the accuracy and speed of aligning the connecting plates. In addition, the system has good environmental adaptability and can operate stably under various light conditions, providing strong technical support for constructing and maintaining trough solar power stations. This study promotes technological progress in solar energy utilization and provides a new solution for industrial automation inspection.*

**Keywords:** solar power technology, image processing, face localization

### 1. Introduction

With the global energy system gradually transitioning towards low carbon and diversification, and the concept of environmental protection deeply penetrating and strengthening across all levels of society, solar energy, due to its clean, non-polluting, and sustainable utilizable characteristics, has become a highly regarded strategic form of renewable energy worldwide [1]. Solar thermal

---

<sup>1</sup> Shaanxi Polytechnic University, Xianyang 712000, Shaanxi, China; Xianyang Key Laboratory of Ultra Precision Digital Gold Cutting and Control, Xianyang 712000, Shaanxi, China. Email: 598914251@qq.com

<sup>2</sup> Shaanxi Polytechnic University, Xianyang 712000, Shaanxi, China; Xianyang Key Laboratory of Ultra Precision Digital Gold Cutting and Control, Xianyang 712000, Shaanxi, China

<sup>3</sup> Shaanxi Polytechnic University, Xianyang 712000, Shaanxi, China; Xianyang Key Laboratory of Ultra Precision Digital Gold Cutting and Control, Xianyang 712000, Shaanxi, China

<sup>4</sup> Shaanxi Polytechnic University, Xianyang 712000, Shaanxi, China; Xianyang Key Laboratory of Ultra Precision Digital Gold Cutting and Control, Xianyang 712000, Shaanxi, China

<sup>5</sup> Shaanxi Polytechnic University, Xianyang 712000, Shaanxi, China; Xianyang Key Laboratory of Ultra Precision Digital Gold Cutting and Control, Xianyang 712000, Shaanxi, China

<sup>6</sup> Shaanxi Polytechnic University, Xianyang 712000, Shaanxi, China

power generation technology, as an important branch of solar energy utilization, shows great potential and market competitiveness in the field of renewable energy generation by virtue of its high reliability and system power generation efficiency [2-3]. However, the overall performance and operational efficiency of parabolic trough solar power systems largely depend on the manufacturing precision, assembly accuracy, and long-term dynamic stability of their key components, especially the precise positioning and assembly of the connecting plate surface of the trough solar thermal collector bracket, which is shown in Fig. 1, and 1-8 is the connecting plate surface of the trough bracket.

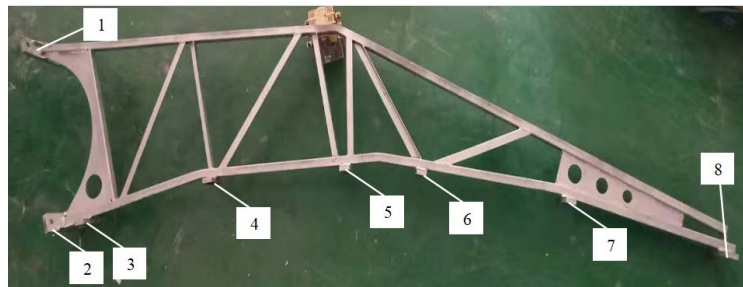


Fig. 1. Physical diagram of the trough bracket

Traditional positioning and detection methods often rely on manual operation, which is inefficient and susceptible to the influence of human factors, resulting in insufficient positioning accuracy, which in turn affects the concentrating efficiency and power generation performance of the entire solar collector system. Therefore, the development of a high-precision, automated, and intelligent positioning system is of great significance for improving the overall performance of the trough solar power generation system and reducing the power generation cost. The application scenarios and advantages of this system are shown in Table 1.

Table 1

Application scenarios and advantages

Application Scenario	Description	Advantage
Assembly of Trough Solar Collector Brackets	Utilized for the precise positioning and assembly of connecting panels	Enhances assembly accuracy, reduces rework expenses
Quality Inspection	Detects dimensions, shapes, etc., of connecting panels to verify compliance with specifications	Improves product quality, lowers defect rates
Production Line Automation Upgrade	Replaces manual operations with automated positioning and inspection systems	Increases production efficiency, cuts labour costs
Remote Monitoring and Maintenance	Remotely monitors system status via network, performs fault alerts, and maintenance.	Boosts system stability, reduces maintenance expenditures.

In recent years, alongside the rapid development of China's solar energy industry, parabolic trough solar thermal power generation technology has attracted wide attention and undergone in-depth research. To address the technical challenge of high-precision spatial positioning of the mounting plate in trough-type solar thermal collector systems, domestic research institutions and industry have, through a collaborative innovation model of industry, academia, and research, systematically carried out technical research on this key link, achieving a series of innovative research results with engineering application value in areas such as positioning algorithm optimization, multi-sensor fusion calibration, and error compensation mechanisms.

In China, scholars mainly focus on selecting and calibrating high-precision industrial cameras, optimizing image processing algorithms, improving the accuracy of mechanical control mechanisms, and system integration and testing [4-5]. By introducing advanced machine learning algorithms and deep learning technologies, domestic researchers have successfully improved the recognition accuracy and positioning speed of the feature points of the connecting plate surface. Meanwhile, domestic enterprises have also made significant progress in designing and manufacturing mechanical control mechanisms, realizing the precise adjustment of the position of the connecting plate surface [6].

Internationally, the trough solar collector bracket connecting plate surface positioning system based on industrial cameras has also received wide attention. Europe, the United States, and other developed countries in solar thermal power generation have a more mature technology accumulation; the research on the connection plate surface positioning system also started earlier. Foreign researchers mainly focus on the innovation of image processing algorithms and optimizing mechanical control mechanisms. By introducing advanced computer vision technology and machine vision algorithms, they have realized the fast and accurate identification of the characteristic points of the connecting plate surface. At the same time, foreign countries have also made significant progress in the mechanical control mechanism, such as high-precision servo motors and transmission mechanisms, etc., to realize the accurate control of the position of the connecting plate surface[7-8].

Therefore, this paper introduces an industrial camera positioning system for the connecting plate surface of a trough solar collector bracket. The system automatically identifies key feature points by integrating image processing technology to position and inspect the connecting plate surface precisely. This system enhances both the accuracy and efficiency of connecting plate alignment. Moreover, it exhibits strong environmental adaptability, enabling stable operation under various lighting conditions. The organization's primary function is to provide technical support for the construction and maintenance of trough-type

solar power stations, thereby facilitating advancement in the field of solar energy utilisation.

## 2. Materials and Methods

For the detection method of the machining accuracy of the connecting plate surface of the slotted bracket, the establishment of a mathematical model is imperative for the investigation of the surface configuration of the connecting plate, to put forward the determination standard, select the surface shape detection device, and design the surface shape detection system. On this basis, if there is an error in the installation position of the laser detection head, it will directly affect the acquisition of data coordinates on the connecting plate of the grooved bracket to be tested, leading to misjudgment of the detection results and affecting the concentrating efficiency of the parabolic concentrating mirror. Therefore, designing an accurate positioning system based on image processing is particularly important for this paper. In this paper, we choose a 2.6mm 130° 4K 5 million pixel  $1.62\mu\text{m}\times 1.62\mu\text{m}$ , boot screen  $2952\times 1944$ , distortion-free USB-type industrial-grade camera for image sampling, and HG-C1030 laser displacement sensor for positioning on the connecting plate surface.

### 2.1 Image Grayscale

In the laser detection system to collect images, on the one hand, we need to consider whether the lens distortion, as well as due to installation errors caused by image distortion and other issues, so this paper selected a 5 million wide-angle distortion-free high-definition industrial cameras, without the need for aberration correction of the camera, only need to consider the installation of the error generated by the link. On the other hand, when shooting the connection plate surface of the slot bracket to be tested, the external environment, the angle of the connection plate position, the flatness of the connection plate, and other factors will lead to unclear image shooting, local noise, and key feature points are not obvious, which in turn affects the matching accuracy of the image. This paper's image preprocessing involves grayscale and noise reduction to eliminate noise, reduce interference, and enhance key image features, improving image quality.

Grayscale converts an original colour image into a grayscale image with a grey scale range of 0-255. Its purpose is to improve recognition efficiency by eliminating the majority of the information in the image irrelevant to the recognition target, making it easier to distinguish the desired content from the background [9]. Since all colour images that computers can present are composed of red, green, and blue colour components, it is necessary to know the compositional relationship between the components of R, G, and B at each pixel point during the grayscale conversion. Commonly used methods of grayscale

conversion are the maximum value method, the average value method, and the weighted average Method.

The maximum value method takes the maximum value of the three colour components of red, green, and blue as the grayscale value (intensity value, brightness value), i.e.  $T = \max(R, G, B)$ , The brightness and darkness of the grayscale image after processing using this Method is harsher; the average value method is to take the average value of the red, green and blue colour components in the pixel points as the grayscale value, that is:

$$T = \frac{1}{3}(R+G+B) \quad (1)$$

This Method will produce a softer grayscale image; the weighted average Method is based on the human eye, on the red, green, and blue three colour components, where the discrimination degree is different, the allocation of the corresponding weight  $w_r$ ,  $w_g$ ,  $w_b$ , and the weight for the average value of the processing, the results of its calculations are regarded as grayscale values, that is:

$$T = \frac{1}{3}(w_r R + w_g G + w_b B) \quad (2)$$

This Method will produce a grayscale image that is most favorable for the human eye to observe. Based on the above comparative analysis, this paper will use the weighted average Method to grayscale the slotted bracket connection plate surface.

## 2.2 Image binarization

Image binarization is a commonly used image preprocessing method. The processing principle is to label all the pixel points on an image according to its grey value after processing to get a grayscale image showing the contours of the objects in the image in black and white. The specific process is first to set a threshold; when the image is processed, the grayscale in the range including the threshold and above the pixel value (with the ability to express the object in the image), the grayscale value will be expressed in 255, and the rest of the pixels (cannot show the characteristics of the object) grayscale value with 0, so that you can present an image through a simple black and white colour. After binarization, the image contains less information, which makes the image simple and straightforward, thus highlighting the target outline and facilitating further processing of the image. Common image binarization includes global fixed thresholding, local adaptive thresholding, and the Otsu method [10].

Among them, the global fixed threshold method is to binarize the whole image using the same threshold, which has a one-size-fits-all effect and is only suitable for binarized image processing with uniform brightness distribution; the

local adaptive threshold method is to calculate the corresponding threshold for binarization according to each region when different parts of an image have different brightness, which can get better-binarized image processing in different brightness situations. This Method can get better-binarized image processing under the situation of different brightness. However, the clarity of pixel extraction is not high enough. As an adaptive threshold segmentation algorithm based on the statistical characteristics of image grayscale, Otsu's Method aims to achieve optimal separation of foreground and background during image binarization by maximizing the inter-class variance between the foreground and background regions. Suppose the inter-class variance of the foreground and background parts is larger. In that case, it represents a greater difference between the two parts of the constituent images, i.e., the smaller the possibility that part of the target is misclassified. Therefore, when the maximum inter-class variance is calculated, it is hypothesized that the current threshold is optimal, and the binarized image at this time is the optimal binarized image, which is simple to calculate, stable, adaptive, and better. Through comparative analysis, this paper will use the Otsu binarization method for the most reasonable binarized image processing.

### 2.3 Edge Detection

An image edge is the set of all pixels where the grey value of the image produces a jump change. The Method of edge detection can reduce the amount of data in the original image, eliminate irrelevant information, and extract the target image contour, which plays a key role in the subsequent conversion of the coordinate system and the laser detector head in the X-axis and Y-axis direction away from the center of the slotted bracket connecting plate to be tested. Standard image edge detection methods include the Sobel edge detection operator, the Laplacian edge detection operator, the Canny edge detection operator, and so on. Among them, the Sobel edge detection operator is based on the characteristic that the grey-level weighted differences of neighbouring pixels in the horizontal and vertical orthogonal directions reach an extreme value in edge regions, thereby achieving detection and localization of image edges [11]. The operation template of this operator is shown in Fig. 2. The image edges extracted by Sobel's edge detection operator have thicker lines and a fuzzy quality.

-1	0	1
-2	0	2
-1	0	1

(a) X-axis direction operator model

-1	-2	-1
0	0	0
1	2	1

(b) Y-axis direction operator model

Fig. 2. Sobel operator model

The Laplacian edge detection operator is a detection method that calculates the second-order derivatives of the image in the horizontal and vertical directions through the Sobel operator, sums the second-order derivatives of the two directions, and compares the results of the calculation with the zero point to determine the edge position [12]. The operator's operation template is shown in Fig. 3. The Laplacian edge detection operator is susceptible to the influence of noise, resulting in partial loss of edge information and local discontinuity of the edge detection results. The Laplacian edge detection operator is susceptible to noise, which leads to the loss of some of the edge information, resulting in a local discontinuity in the edge detection results.

0	1	0
1	-4	1
0	1	0

(a) 4-neighbourhood operator model

1	1	1
1	-8	1
1	1	1

(b) 8-neighbourhood operator model

Fig. 3. Laplacian operator model

The Canny edge detection operator is based on the Gaussian function model and uses dual thresholding to detect strong and weak edges, respectively. The edge detection process is then concluded by suppressing those remaining isolated weak edges. The first-order differential convolution operation template of this operator is shown in Fig. 4. The Canny edge detection operator has high accuracy, low error rate, effective noise suppression, and can accurately locate the edge position of the target object.

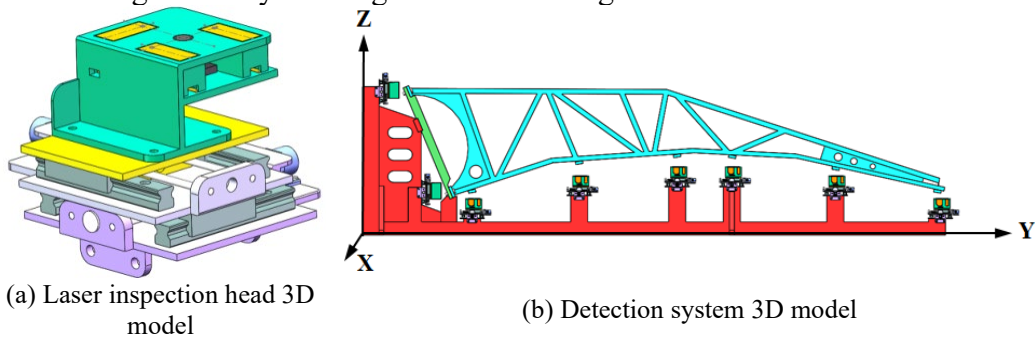
-1	1	1	1
-1	1	-1	-1

Fig. 4. Canny operator model

### 3. Experimental design and procedure

#### 3.1 Experimental platform construction

SolidWorks 3D drawing software is used to carry out solid modeling and assembly of the whole testing experimental platform, display the assembly process, and find out the problems in the assembly in the simulation stage, verify the reasonableness of the assembly design of the experimental platform, so that the researcher can make timely modifications to the 3D model, and get the final 3D modeling assembly drawing. As shown in Fig. 5.

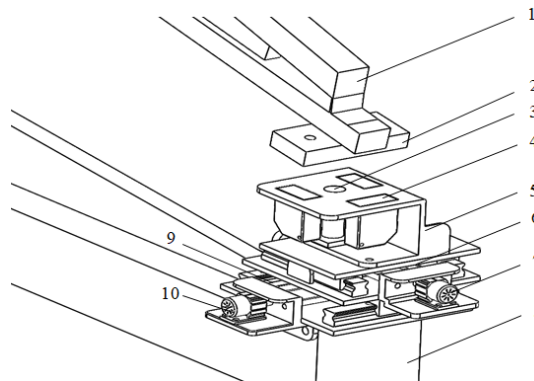


(a) Laser inspection head 3D model

(b) Detection system 3D model

Fig. 5. Experimental platform 3D modeling assembly diagram

The size of the laser inspection head, installation position, processing accuracy, detection accuracy, external environment, and other factors will directly affect the data detection of the slot bracket connecting the plate surface. The laser inspection head designed in this paper consists of three parts: a camera positioning module, a laser displacement sensor data acquisition module, and a cross slide module, as shown in Fig. 6. Among them, the camera positioning module is installed in the center of the detector head bracket through MATLAB image processing and PLC offset control, so that the center of the laser detector head and the center of the slotted bracket connection plate can be tested.



1-Trough solar collector bracket; 2-Trough bracket connecting plate; 3-Industrial camera;  
4-Laser displacement sensor; 5-Inspection head bracket; 6-X-axis slider; 7-X-axis drive motor;  
8-Inspection bench frame; 9-Y-axis slider; 10-Y-axis drive motor

Fig. 6. 3D model of laser inspection head

The installation position of the three laser displacement sensors in the laser displacement sensor data acquisition module needs to satisfy the relationship shown in Fig. 7; that is, the laser emission interface of two of the sensors is in a horizontal line with the center of the industrial camera, and in the direction of the plumb line of this horizontal line there is another sensor's laser emission interface is also in a horizontal line with the center of the industrial camera. The cross-slide module controls the X-axis and Y-axis direction movement and adjusts the offset. The purpose is to mount the laser detector head above the cross-slide table and test the center position of the connecting plate of the bracket to complete the positioning operation.

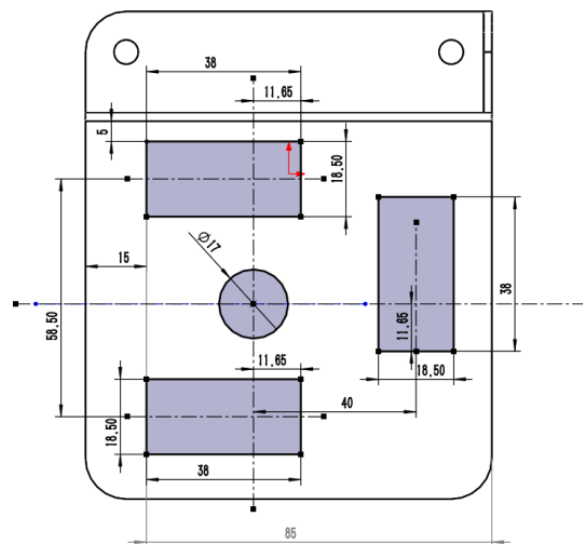


Fig. 7. Layout of the upper surface position of the inspection head

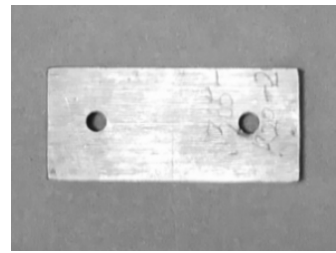
## 3.2 Image processing experiments

### 3.2.1 Image processing method

Based on the theoretical comparative analysis, this experiment aims to convert the colour image of the connecting plate surface of the slotted bracket into a grayscale image. First, the colour image of the connecting plate surface is captured; then, according to the sensitivity of the human eye to different colours, the weights are assigned to the red, green, and blue colour components; then, the grayscale value of each pixel is calculated by using the weighted average Method; finally, the calculated grayscale value is assigned to the corresponding pixel to generate a grayscale image. Standard greyscale conversion methods include the maximum value method, the average value method, and the weighted average Method. This paper will use the weighted average Method for grayscale processing<sup>[13]</sup>, as shown in Fig. 8.



(a) Original image



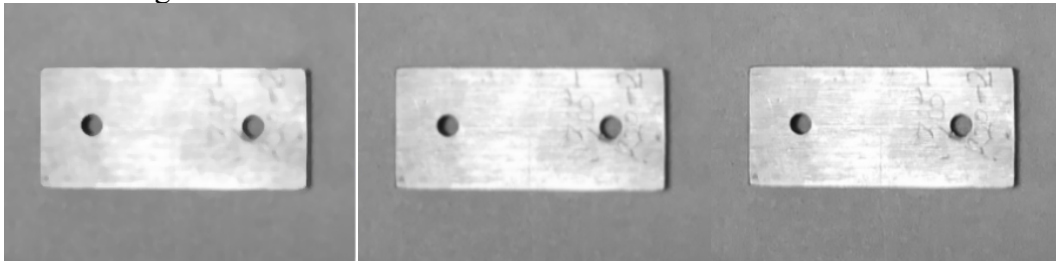
(b) Grayscale conversion using the weighted averaging method

Fig. 8. Grayscale comparison diagram

Due to the shooting environment, shooting duration, and leakage current, interference to the camera's internal sensor will occur, causing the laser detector head to produce mechanical micro-vibration, which generates Gaussian noise, thermal noise, pretzel noise, and so on. Therefore, image noise reduction processing can reduce the noise in digital image. Commonly used image noise reduction methods are mean filtering, adaptive Wiener filtering, median filtering, and so on [14-16].

Among them, the mean filtering method uses the neighbourhood averaging Method to replace the grayscale average of several pixels with each pixel's grayscale value. This Method is suitable for removing granular and Gaussian noise, but the processed image is easily distorted. The Adaptive Wiener filtering method uses the local variance method to minimize the mean square deviation of the image before and after processing. The Method is good at dealing with white noise and is effective in processing images with motion blur, but the algorithm is computationally extensive. The median filtering method calculates the median of the values of the points in a field at a certain point in a digital image or a sequence, and replaces the point with the median value. The Method is good at dealing with

pepper noise, the algorithm is simple, the time complexity is low, and the image edge contour is not distorted. Three commonly used noise reduction methods are shown in Fig. 9.



(a) Mean filtering method      (b) Adaptive Wiener filtering method      (c) Median filtering method

Fig. 9. Noise reduction effect diagram

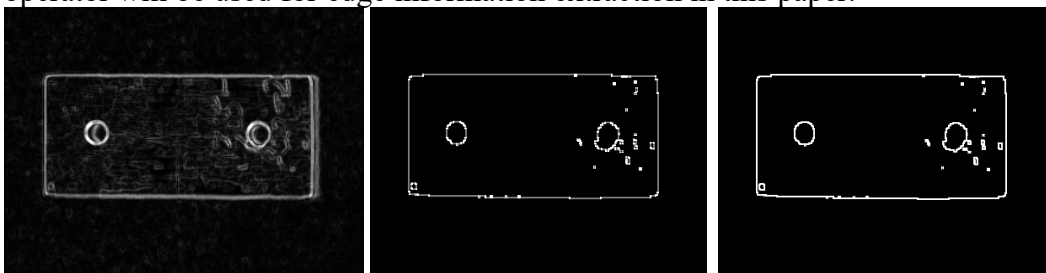
Through experimental comparison, this paper will use the Otsu binarization method for the most reasonable binarization image processing. Three commonly used binarization processing methods are shown in Fig. 10<sup>[17]</sup>.



(a) Global fixed threshold method      (b) Local adaptive threshold method      (c) Otsu method

Fig. 10. Binarization effect diagram

As shown in Fig. 11, by comparing the various algorithms, it can be obtained that the Canny edge detection operator recognizes the image contours more clearly and with higher accuracy [18]. Therefore, this edge detection operator will be used for edge information extraction in this paper.



(a) Sobel operator      (b) Laplacian operator      (c) Canny operator

Fig. 11. Edge detection effect diagram

### 3.2.2 Method comparison

To achieve high-precision positioning, it is necessary to quantitatively evaluate the geometric errors that may be introduced at each stage of image processing. This paper employs the reprojection error as the core evaluation metric, defined as the root mean square error (RMSE) of the Euclidean distance between the coordinates of feature points extracted through image processing and reprojected back into physical space, and known standard target points. Let the standard target point set be  $\{P_i^{true}\}_{i=1}^N$ , and the estimated point set obtained after

image processing and coordinate transformation be  $\{P_i^{est}\}_{i=1}^N$ . Then, the

reprojection error is  $\mathcal{E}_{rep} = \sqrt{\frac{1}{N} \sum_{i=1}^N \|P_i^{true} - P_i^{est}\|^2}$ . This metric effectively reflects the impact of the entire image processing chain on geometric information fidelity, enabling fair comparisons between different algorithms.

#### (1) Influence of greyscale methods on error

Aiming at the graying stage, the same group of original images is processed by the Mum Method, the age Method, and the weighted average Method (the weight coefficient is in accordance with the R BT.601 standard  $\omega_R = 0.299$ ,  $\omega_G = 0.587$ ,  $\omega_B = 0.114$ ), and then median filtering, Otsu binarization, and Canny edge detection are adopted. The experimental results show that the weighted average Method is the best in terms of stability of feature point extraction, and its average reprojection error is 0.182mm, which is significantly lower than the maximum Method (0.247mm) and the average Method (0.215mm), as shown in Table 2. This is because the weighted average better aligns with human visual response characteristics, preserving more structural details and facilitating precise edge localization in subsequent steps.

Table 2

Reprojection error under different grey scaling methods (unit: mm)

Method	Mean Error	Standard Deviation
Maximum value method	0.247	0.031
Mean value method	0.215	0.025
Weighted average method	0.182	0.018

#### (2) Impact of Noise Reduction Methods on Error

Under fixed greyscale conversion conditions, the effects of mean filtering(window size  $5 \times 5$ ), adaptive Wiener filtering, and median filtering

(window size  $5 \times 5$ ) on positioning accuracy were compared. Experiments demonstrated that median filtering effectively suppressed salt-and-pepper noise while preserving edge sharpness, yielding the lowest reprojection error (0.182 mm). Whilst mean filtering smooths Gaussian noise, it causes edge blurring, increasing the error to 0.236 mm. Wiener filtering, which calculates local statistical properties, exhibits instability under non-stationary noise, yielding an error of 0.209 mm and increasing computational time by approximately 3.2 times. As shown in Table 3.

Table 3

**Reprojection error under different denoising methods (unit: mm)**

Method	Average Error	Processing Time (ms/frame)
Mean Filter	0.236	8.2
Adaptive Wiener filter	0.209	26.5
Median filtering	0.182	9.1

(3) Effect of Binarisation Methods on Error

Under identical preprocessing conditions, three binarisation strategies were compared. The global thresholding method, unable to adapt to uneven illumination, resulted in feature loss in certain regions, with an error of 0.274 mm. The local adaptive thresholding method, whilst improving robustness to illumination variations, introduced edge jitter due to threshold fluctuations, resulting in an error of 0.210mm. Conversely, the Otsu method automatically determines the globally optimal threshold by maximising inter-class variance. In the experimental scenario, this yielded the most stable binary contours, reducing the error to 0.182 mm, as shown in Table 4.

Table 4

**Reprojection error under different binarisation methods (unit: mm)**

Method	Average Error	Edge Continuity Score(1-5)
Global Fixed Threshold Method	0.274	2.1
Local adaptive thresholding method	0.210	3.8
Otsu's method	0.182	4.6

#### (4) Influence of edge detection operators on error

Finally, under a unified preprocessing workflow, the localization performance of the Sobel, Laplacian, and Canny operators was compared. The Sobel operator, utilising only first-order derivatives with a simple template, produced coarse edges with an error of 0.228 mm. The Laplacian operator is sensitive to noise and prone to producing discontinuous edges, with an error of 0.251 mm. The Canny operator, however, effectively balances noise suppression and precise edge localization through Gaussian smoothing, non-maximum suppression, and dual-threshold hysteresis. This results in a final error of merely 0.182 mm and the most continuous edges. As shown in Table 5.

Table 5

Reprojection error under different edge detection operators (unit: mm)

Operator	Average Error	Edge Localisation StandardDeviation (pixels)
Sobel	0.228	0.87
Laplacian	0.251	1.12
Canny	0.182	0.43

The combined strategy of weighted average greyscaling, median filtering for noise reduction, Otsu's thresholding, and Canny edge detection achieved the smallest reprojection error (0.182 mm) across all test scenarios. Furthermore, the error contributions from each stage were mutually compatible, exhibiting no significant cumulative amplification effect. This combination not only meets the sub-millimeter positioning accuracy requirement for channel-type bracket connection plates (engineering tolerance  $\leq 0.3$  mm) but also demonstrates excellent real-time performance and robustness.

#### 4. Experimental analysis report

After completing the edge detection work, use the MATLAB camera calibration to ensure that the industrial camera and the slot bracket to be tested in the center of the board surface are square, and complete the camera positioning operation.

This experiment is based on the feature extraction technique of Hough Transform by quantizing the Hough parameter space into finite intervals, which is

used to realize the transformation when the slope parameter does not exist or is infinite in straight line detection in order to realize the task of contour extraction of the final target image [19-20]. Based on the camera calibration module in MATLAB's Computer Vision Toolbox, the camera imaging model parameters are calibrated using a high-precision chessboard calibration method. The camera intrinsic parameter matrix is obtained through corner detection and optimization algorithms on multi-view chessboard images. Combined with the actual pose data of the camera in three-dimensional space, the camera extrinsic parameter matrix is calculated using rigid body transformation theory. Furthermore, using homogeneous coordinate transformation, precise mapping between the world coordinate system, camera coordinate system, and image coordinate system is achieved, ultimately obtaining the high-precision extraction results of the target contour in the camera coordinate system, as shown in Fig. 12.

The above camera coordinate system under the contour extraction map is converted to the world coordinate system and then marked with a blue star where the camera is located; its coordinates are (0,0), and then calculate the slot bracket connected to the center of the plate shape is located, expressed in red stars, its coordinates are (-4.07,-2.31), the final result is shown in Fig. 13. In summary, based on the camera positioning system in this chapter, the processing of the image can be obtained: when the industrial camera, that is, the laser detector head forward 2.31mm, and then to the left 4.07mm, the industrial camera can be with the groove bracket to be tested in the center of the plate surface to be right, to complete the camera positioning operation.

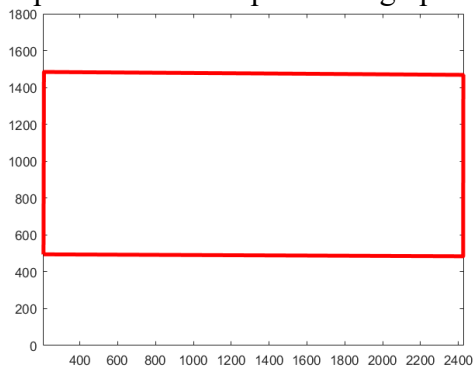


Fig. 12. Edge contour extraction in the camera coordinate system

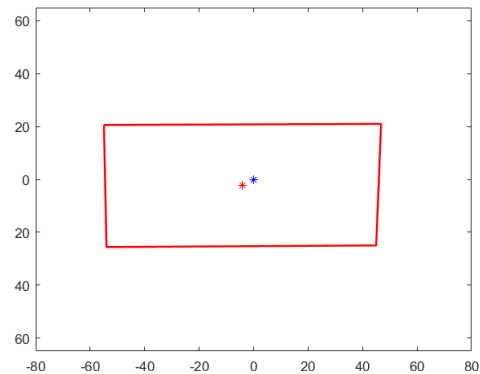


Fig. 13. Final positioning diagram

The novelty of this study lies in the development of an error-driven, customized image processing pipeline specifically tailored to address the challenges posed by low-texture and highly reflective surfaces of channel-type bracket connection plates. By quantitatively evaluating grey scaling, denoising, binarisation, and edge detection methods, an optimal combination was established and rigorously validated—using reprojection error as the primary metric—to achieve sub-millimeter positioning accuracy (0.182 mm). Rather than proposing a

novel algorithm, this work systematically selects, coherently integrates, and holistically optimizes existing, well-established techniques to formulate a highly robust, quantifiable, and reproducible visual localization solution. This approach demonstrably outperforms conventional generic processing strategies and effectively fulfils the stringent requirements for high-precision automated assembly of parabolic trough solar collectors.

## 5. Conclusion

This paper addresses the high-precision localization requirement for the connector plates of parabolic trough solar collector support structures by designing and implementing a vision-based localization system employing industrial cameras. By optimizing both the image acquisition configuration and the subsequent processing pipeline, the system effectively mitigates interference caused by low surface texture, strong specular reflections, and variations in ambient illumination, thereby providing a reliable geometric data foundation for downstream automated manufacturing and quality inspection processes.

In this work, the imaging setup was rationally configured based on the structural characteristics of the support brackets and the performance specifications of the industrial camera. Through systematic experimentation, an optimal image processing pipeline was established, comprising weighted-average greyscale conversion, median filtering for noise suppression, Otsu's Method for binarisation, and Canny edge detection. Quantitative evaluation demonstrates that, under standard test conditions, the proposed pipeline achieves a mean reprojection error of 0.182 mm, satisfying the engineering tolerance requirement ( $\leq 0.3$  mm) and significantly outperforming conventional generic processing strategies.

Furthermore, the system exhibits excellent repeatability across multiple experimental trials, with a pixel-level standard deviation of only 0.43 in edge localization, and maintains consistent performance under varying lighting conditions, confirming its robustness. By integrating a high-resolution industrial camera, high-quality optical lenses, and an error-driven optimized algorithmic pipeline, the developed system delivers quantifiable accuracy, high stability, and engineering-grade reliability. This approach provides an effective technical solution for enhancing both manufacturing efficiency and product consistency in the production of parabolic trough solar collectors.

## Acknowledgements

2024 Xianyang Key Laboratory-Xianyang Ultra-precision Digital Metal Cutting and Control Key Laboratory (Project No.: S2024-KCPT-ZDSYS-2723); Key scientific research project of Shaanxi University of Technology in 2025 (Project No.: 2025 YKZD-005); Youth Science and Technology Innovation Team of Shaanxi University of Technology in 2025 (Project No.: KCTD2025-01); Innovation Capability Support Program of Shaanxi (Project No.: 2025CG-GNYZZ-07); Intelligent Financial Auditing and Cost Traceability through Collaborative Integration of Visual Information and Sensor Data (Project No.: 25JK0319)

## REFERENCES

- [1] *Li P, Cheng J, Yang Y, et al.*, Research on multi-objective optimization configuration of solar ground source heat pump system using data-driven approach. *Energy*, 2024, 313133793-133793.
- [2] *Almohammadi K, Allouhi A.*, Techno-economic assessment and optimization of grid-connected solar PV systems in Saudi Arabia's building sector. *Utilities Policy*, 2025, 93101885-101885.
- [3] *Almohamed H N, Ali M W S.*, Concentrated Solar Thermal-Thermoelectric generator hybrid systems: Review the Most Recent Developed technologies. *IOP Conference Series: Earth and Environmental Science*, 2025, 1440(1):012008-012008.
- [4] *Zhou B, Li A X.*, Particle breakage behavior of silty loess: Insights based on experimental tests, image analysis, and numerical simulation. *Engineering Geology*, 2025, 346107904-107904.
- [5] *Kordnoori S, Sabeti M, Mostafaei H, et al.*, Cutting-edge multi-task model: unveiling COVID-19 through fusion of image processing algorithms. *Computer Methods in Biomechanics and Biomedical Engineering: Imaging & Visualization*, 2024, 12(1).
- [6] *Yang Y.*, Automatic control technology of mechanical equipment based on microelectronic sensing signal control. *International Journal of Modern Physics C*, 2024, (prepublish).
- [7] *Huynh T V, Lim P C, Najdovski Z, et al.*, Minimal operation region prediction for networked control robotic manipulators subject to time-varying delays and disturbances. *IET Control Theory & Applications*, 2024, 18(8):1085-1097.
- [8] *Arezoo K, Arezoo J, Tarvirdizadeh B, et al.*, Modeling and control of robotic manipulators equipped with the flexible cable-pulley based gravity compensation mechanism. *Journal of Vibration and Control*, 2024, 30(7-8):1524-1547.
- [9] *Liu J, Fang F, Du N.*, Color-To-Gray Conversion with Perceptual Preservation and Dark Channel Prior. *Int. J. Numer. Anal. Mod.*, 2019, 16(4):668-679.
- [10] *Villarreal R, Solano C S, Cantillo S, et al.*, An innovative methodology for segmenting vessel like structures using artificial intelligence and image processing. *Scientific reports*, 2024, 14(1):30332.
- [11] *Wang Y, Yin T, Chen X, et al.*, A steel defect detection method based on edge feature extraction via the Sobel operator. *Scientific Reports*, 2024, 14(1):27694-27694.
- [12] *Suzhen Y, Wenhao Z, D. J D, et al.*, Quantum image edge detection based on Laplacian of Gaussian operator. *Quantum Information Processing*, 2024, 23(5).
- [13] *Liqin C, Lei J, Zhijiang L, et al.*, Grayscale Image Colorization Using an Adaptive Weighted Average Method. *Journal of Imaging Science and Technology*, 2017, 61(6): 605021-6050210.

- [14] *Devapal D, Kumar S S, Jojy C.*, A Novel Approach of Despeckling SAR Images Using Nonlocal Means Filtering. *Journal of the Indian Society of Remote Sensing*, 2017, 45(3):443-450.
- [15] *Tang C.*, Noise Reduction Method of Adaptive Wiener Filtering for Ocean Remote Sensing Image. *Journal of Coastal Research*, 2018, 83(sp1):651-655.
- [16] *Adiputra I P, Akbar A L.*, Grayscale Image Quality Analysis Result of Noises Reduction using Adaptive Fuzzy Filter (AFF) and Spatial Median Filter (SMF) Against Image Depth Variations. *Journal of Physics: Conference Series*, 2019, 1361012024-012024.
- [17] *Min-kyung K, Yoon-soo Y, Hyun-joon S.*, Binarization for eliminating calibration in fiberscope image processing. *Optics Communications*, 2021, 497
- [18] *Maranga O J, Nnko J J, Xiong S.*, Learned active contours via transformer-based deep convolutional neural network using canny edge detection algorithm. *Signal, Image and Video Processing*, 2025, 19(3):222-222.
- [19] *Sandra M, Faris E, Amani A, et al.*, An automatic image processing based on Hough transform algorithm for pavement crack detection and classification. *Smart and Sustainable Built Environment*, 2025, 14(1):1-22.
- [20] *Rahman S, Ramli M, Arnia F, et al.*, Analysis and Comparison of Hough Transform Algorithms and Feature Detection to Find Available Parking Spaces. *Journal of Physics Conference Series*, 2020, 1566(1):012092.